Unsymmetrical one-electron oxidized Ni(ii)–bis(salicylidene) complexes: a protonation-induced shift of the oxidation site†

Amélie Kochem,[a] Maylis Orio,[b] Olivier Jarjayes,*[a] Frank Neese[b] and Fabrice Thomas*[a]

The spin density in the nickel(ii) radical salen complex $(2^{\bullet})^{+}$ could be localized on a specific ring by controlling the acidity of the medium.

The cooperativity between metals and radicals allows a high level of both sophistication and performance in biocatalysis.[1] In order to better understand the properties of this peculiar entity many complexes involving coordinated radicals have been synthesized.[2] The most recent advances in this field have been achieved with nickel(ii)-radical salen complexes. Indeed, such compounds exhibit interesting valence tautomerism properties promoted by external stimuli (the nickel(ii)-radical form is for instance converted into the nickel(iii)-phenolate form in the presence of coordinating solvent),[3,4] whereas the first X-ray crystal structures of nickel(ii)-radical species were solved in 2007[5] and 2010.[6] A striking feature in the two crystal structures is the quite different spin density distribution. From the analysis of the bond lengths within the rings, $(1^{tBu\bullet})^{+}$ (Fig. 1) was found to be a fully delocalized radical complex—i.e. the SOMO is equally distributed over the two rings[5]—whereas the SOMO was found to be localized on a single phenoxyl ring in $(1^{OMe\bullet})^{+}$ (Fig. 1).[6] Understanding the

parameters that govern the localized vs. delocalized character of the radical is a topic of current interest in the coordination chemistry of odd-electron compounds. Herein, we describe two successors to $(1^{OMe\bullet})^{+}$, namely **2** and $(2H)^{+}$, which were synthesized from an unsymmetrical salen ligand (Fig. 1). We show in this report that the SOMO of the radical species can be localized at a specific ring of the molecule by controlling the acidity of the medium.

The nickel complex $(2H)^{+}$ has been obtained by reacting the 2-[(2-amino-phenylimino)-methyl]-4,6-di-tert-butyl-phenol[7] with the 3-tert-butyl-5-dimethylamino-2-hydroxy-benzaldehyde in the presence of Ni(ClO$_4$)$_2$·6H$_2$O.‡ **2** was generated in situ by the addition of NEt$_3$ to $(2H)^{+}$.

2 exhibits a ligand band at 386 nm (21 300 M^{-1} cm^{-1}) in its electronic spectrum as well as a phenolate-to-metal charge transfer transition at 507 nm (6440 M^{-1} cm^{-1}). These bands are blue-shifted in $(2H)^{+}$ (379 nm (20 900 M^{-1} cm^{-1}) and 490 nm (6690 M^{-1} cm^{-1})), in agreement with a lowering of the electron-donating properties of a phenolate substituent,[8] and thus protonation of the N-dimethylamine (Fig. S1, ESI†).

The cyclic voltammetry (CV) curve of **2** (Fig. 2) displays a reversible one-electron oxidation wave at $E_{1/2}^{1} = -0.14$ V, as well as a signal at $E_{1/2}^{2} = 0.55$ V. The former is attributed to the oxidation of the N,N-dimethylaminophenolate moiety into a N,N-dimethylaminophenoxyl radical, whereas the second is ascribed to the di-tert-butylphenoxyl/di-tert-butylphenolate redox couple. The $E_{1/2}^{1}$ value is found to be similar to the one reported for 3^{NMe} (Fig. 1), which features two equivalent N-dimethylaminophenolate moieties ($E_{1/2}^{1} = -0.14$ V, $E_{1/2}^{2} = 0$ V), whereas $E_{1/2}^{2}$ is close to the $E_{1/2}^{1}$ value reported for 3^{tBu} (0.58 V).[8] This suggests that spin sharing in $(2^{\bullet})^{+}$ is weak. In the case of $(2H)^{+}$ the oxidation wave is shifted
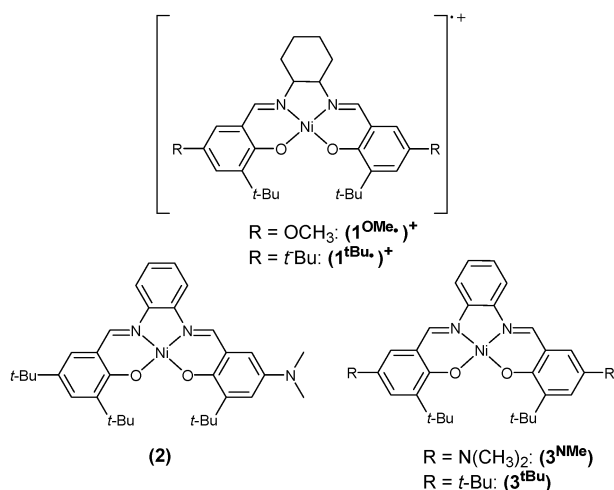
Fig. 1 Complexes of interest in this study.

R = OCH$_3$: $(1^{OMe\bullet})^{+}$
R = tBu: $(1^{tBu\bullet})^{+}$

(2)

R = N(CH$_3$)$_2$: (3^{NMe})
R = t-Bu: (3^{tBu})

[a] Département de Chimie Moléculaire,
Chimie Inorganique Redox Biomimétique (CIRE),
UMR CNRS 5250, Université J. Fourier, B. P. 53
38041 Grenoble cedex 9, France
E-mail: Fabrice.Thomas@ujf-grenoble.fr; Fax: +33 476 514 836;
Tel: +33 476 514 373
[b] Institute for Physical and Theoretical Chemistry - Universität Bonn,
Wegelerstraße 12, 53113 Bonn, Germany
† Electronic supplementary information (ESI) available: UV-Vis, EPR spectra, spin density plots and calculated hyperfine coupling constants. See DOI: 10.1039/c0cc01775b
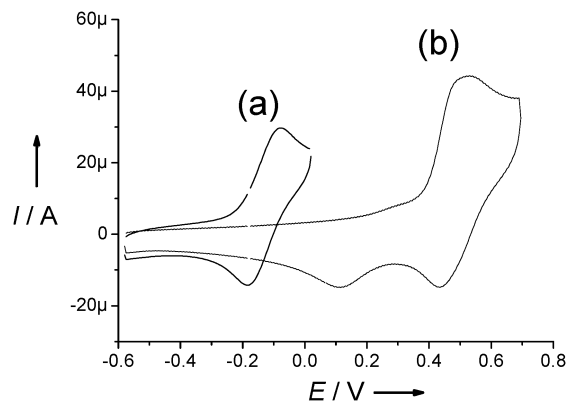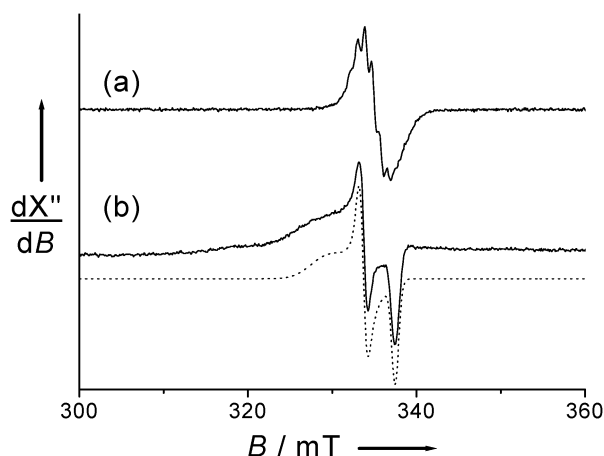

Fig. 2 Cyclic voltammetry curves of 1 mM solutions of complexes **2** (a) and $(2H)^{+}$ (b) in CH$_2$Cl$_2$ solution (+0.1 M TBAP). Scan rate: 0.1 V s^{-1}, T = 298 K. The potentials are referenced versus the Fc/Fc^{+} couple.

towards the anodic region of potentials ($E_{1/2}^1$ = 0.47 V, Fig. 2 and Fig. S2 and S3, ESI†). The limited chemical reversibility of the oxidation wave of $(2H)^+$ when compared to **2** also suggests a lower stability of the oxidized species. The increase in $E_{1/2}^1$ reveals a shift in the oxidation locus from the 2-*tert*-butyl-4-dimethylaminophenolate to the 2,4-di-*tert*-butyl-phenolate moiety (*vide supra*). Indeed, protonation occurs on the *N*-dimethylamine, making this substituent strongly electron-withdrawing and thus less prone to stabilize phenoxyl radicals. Accordingly, the $E_{1/2}^1$ obtained for $(2H)^+$ resembles the value reported for the symmetrical 3^{tBu}.[4]

The one-electron oxidized $(2^•)^+$ has been generated electro-chemically in CH_2Cl_2 (+0.1 M TBAP). Its electronic spectrum differs from the one of **2** (Fig. S4, ESI†) by the splitting of the 386 nm absorption band into two components at 360 nm (19 600 M^{-1} cm^{-1}) and 378 nm (20 100 M^{-1} cm^{-1}) and the appearance of a new band at 624 nm (7750 M^{-1} cm^{-1}). Similar features were observed in the visible spectrum of the radical species $(3^{NMe•})^+$ (630 nm, 7890 M^{-1} cm^{-1}),[8] thus confirming that oxidation takes place on the *N,N*-dimethylaminophenolate moiety. The electronic spectrum of $(2H^•)^{2+}$ is dominated by a band at 355 nm (12 000 M^{-1} cm^{-1}) with shoulders at 464 nm (6680 M^{-1} cm^{-1}) and 569 nm (3500 M^{-1} cm^{-1}). These features are quite different to those characterizing $(2^•)^+$ or $(3^{NMe•})^+$, but fairly close to those reported for $(1^{tBu•})^+$. In addition, while $(2^•)^+$ is relatively stable (half-life of 152 min at 298 K, Fig. S5†), $(2H^•)^{2+}$ is found to decompose quickly, even at 243 K. These results are consistent with a shift of the electronic hole from the 4-*N,N*-dimethylamino-2-*tert*-butylphenoxyl to the 2,4-di-*tert*-butylphenolate moiety when the dimethylamino substituent is protonated. Indeed, *para tert*-butyl groups do not stabilize phenoxyl radical species so efficiently than *N,N*-dimethylamino substituents.
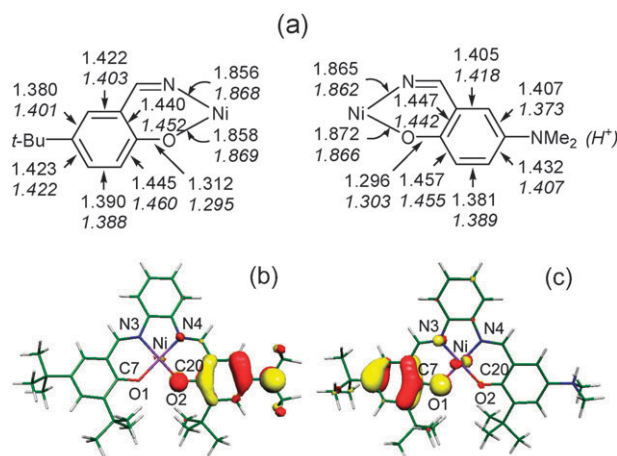
In order to obtain insight into the electronic and geometric structures of the radical complexes $(2^•)^+$ and $(2H^•)^{2+}$, EPR measurements and DFT calculations were undertaken.‡

The 100 K X-band EPR spectrum of $(2^•)^+$ in CH_2Cl_2 (+0.1 M TBAP) is depicted in Fig. 3. It is characterized by an almost isotropic ($S = \frac{1}{2}$) signal centered at $g_{iso} \approx 2.01$, with a hyperfine splitting that is attributed to the interaction of the unpaired electron spin with the *N,N*-dimethylamino substituent. The following hyperfine coupling (HFC) constants were obtained from the simulation of the EPR spectrum in fluid solution at 223 K (Fig. S6, ESI†): A^1_H = 23.0 MHz (6H, two methyl groups of the N(CH$_3$)$_2$), A_N = 13.2 MHz, A^2_H = 28 MHz mT and A^3_H = 10.1 MHz (g_{iso} = 2.006).[9] The existence of the large HFC constants A^1_H and A_N indicates that a significant amount of spin is delocalized onto the *N,N*-dimethylamino group. In addition, the g_{iso} value is very close to those reported for zinc-phenoxyl radical salen complexes, which indicates that the radical is almost purely ligand-based, as previously reported for $(3^{NMe•})^+$. Interestingly, this g_{iso} value is nicely reproduced by DFT calculations (computed g_{iso} of 2.006), and the g-tensor anisotropy is calculated as g_1 = 1.997, g_2 = 2.007 and g_3 = 2.013. The frozen solution EPR spectrum of $(2H^•)^{2+}$ in CH_2Cl_2 exhibits a strongly anisotropic ($S = \frac{1}{2}$) signal at g_1 = 1.994, g_2 = 2.017, and $g_3 \approx 2.045$ ($g_{iso} \approx 2.02$). This set of g-values is, again, in very good agreement with the one predicted by DFT calculations (g_1 = 1.994, g_2 = 2.016, g_3 = 2.037, g_{iso} = 2.016) for localization of the radical on the di-*tert*-butylated ring. In addition, they are close to those reported for the symmetrical radical complex $(3^{tBu•})^+$ (g_1 = 1.991, g_2 = 2.014, $g_3 \approx 2.06$ (broad)).[8] The significant deviation of the g_{iso} value from *ca.* 2.005 (the expected value for a free phenoxyl radical) results from a non-negligible contribution of a metal orbital to the SOMO (*vide supra*).[3–6] It is noteworthy that the similarity between the EPR spectra of $(2H^•)^{2+}$ and $(3^{tBu•})^+$ suggests that either the radical is developed on a single ring in the latter complex, or delocalization over both rings does not contribute significantly to the g-tensor anisotropy.

The structural features of $(2^•)^+$ and $(2H^•)^+$ have been predicted by DFT geometry optimizations (Fig. 4a). A striking feature in the structure of $(2^•)^+$ is the non-equivalence of the Ni–O bond distances, the Ni–O2 bond being larger by 0.014 Å

Fig. 3 X-Band EPR spectra of 1 mM CH_2Cl_2 solutions (containing 0.1 M TBAP) of $(2^•)^+$ (a) and $(2H^•)^{2+}$ (b). Solid lines are experimental spectra, dotted lines a simulation using the parameters given in the text. T = 100 K, microwave frequency 9.42 GHz, power 20 mW, modulation frequency 100 KHz, amplitude 0.04 mT (a) and 0.16 mT (b).

Fig. 4 (a) Bond distances (Å) from geometry optimization in the phenolate/phenoxyl rings of $(2^•)^+$ (normal text) and $(2H^•)^{2+}$ (italic text) (only the *para*-substituent is shown for the sake of clarity) and localized SOMOs for $(2^•)^+$ (b) and $(2H^•)^{2+}$ (c).

with respect to the Ni–O1 one. In addition, a quinoidal distortion of the C–C bonds was calculated within the *N,N*-dimethylamino substituted ring (shorter C–O and C_{ortho}–C_{meta} bonds as well as longer C_{meta}–C_{para} bonds). These features indicate that the radical is indeed localized preferentially on one side of the molecule,[6] more specifically on the 4-*N,N*-dimethylamino-2-*tert*-butylphenoxyl ring. By comparing the Ni–O1 bond lengths in $(2^{\bullet})^{+}$ and $(2H^{\bullet})^{+}$ one notices that a larger value is obtained in the latter case. In addition, the Ni–O2 bond in $(2^{\bullet})^{+}$ is found to be longer than in $(2H^{\bullet})^{+}$. This evidences a shift in the oxidation locus, a fact that is confirmed by the quinoidal distortion found in the di-*tert*-butylated ring in $(2H^{\bullet})^{+}$.

The spin population analysis further supports that oxidation of **2** occurs specifically on the 4-*N,N*-dimethylamino-2-*tert*-butylphenolate moiety. Indeed, the spin-density map (Fig. S8, ESI†) shows positive spin populations in this ring (accounting for 85% of the total spin density), whereas no significant spin density was obtained on the adjacent fragment. The individual contributions were calculated to be O2 (0.15), C20 (0.10), C_{meta} (0.17), C_{para} (0.10) and *para-N*-dimethyl (0.33). In the case of $(2H^{\bullet})^{2+}$, the spin density appears to be mainly localized on the di-*tert*-butylated ring, with positive spin populations at O1 (0.24), C7 (0.10), C_{ortho} (0.16, 0.15) and C_{para} (0.25). Further evidence of the shift of electronic hole on going from $(2^{\bullet})^{+}$ to $(2H^{\bullet})^{2+}$ could be obtained from the composition of the SOMOs (Fig. 4b and c). Both are delocalized π-orbitals that are mainly developed on one specific aromatic ring. Interestingly, a contribution from a d_{yz} orbital to the SOMOs could be evidenced in both cases, whose magnitude is 2% and 8% for $(2^{\bullet})^{+}$ and $(2H^{\bullet})^{2+}$ respectively. Therefore, while the SOMO is mainly hosted by the ligand in $(2^{\bullet})^{+}$, there is a substantial contribution of a metal orbital in $(2H^{\bullet})^{2+}$. Such a change is ascribed to the extra delocalization of the radical in the *N,N*-dimethylamino group of $(2^{\bullet})^{+}$. A direct consequence of this enhanced metal contribution to the SOMO is an increase in the g_{iso} value, which is both predicted theoretically and experimentally observed (*vide infra*).

In conclusion, the radical of $(2^{\bullet})^{+}$ is specifically distributed on the 4-*N,N*-dimethylamino-2-*tert*-butylphenoxyl moiety. No communication exists between the aromatic rings of $(2^{\bullet})^{+}$. Protonation of the *N,N*-dimethylamino induces a significant spin redistribution: in $(2H^{\bullet})^{2+}$ the radical is mainly hosted by the opposite ring (2,4-di-*tert*-butylphenoxyl) and a non-negligible (8%) contribution of the metal to the SOMO could be evidenced.

Notes and references

‡ Synthesis of $(2H)^{+}(ClO_4)^{-}$: to a yellow solution of salicylidene (1-iminophenylene-2-amine)[7] (0.162 g, 0.5 mmol) dissolved in MeOH (10 mL) was added $Ni(ClO_4)_2 \cdot 6H_2O$ (0.1825 g, 0.5 mmol) in MeOH (5 mL). After 10 minutes of stirring, a solution of 3-*tert*-butyl-2-hydroxy-5-*N*-dimethylbenzaldehyde[8] (0.110 g, 0.5 mmol) dissolved in MeOH (2 mL) was added to the resulting red solution. The solution was stirred at reflux for 1 h 30 min and the resulting dark red precipitate was filtered and washed with cold MeOH and diethyl

ether. Yield: 0.175 g (60%). Anal. calcd for $C_{34}H_{44}ClN_3O_6Ni$: C, 59.63; H, 6.48; N, 6.14; Cl, 5.18; Ni, 8.57%. Found: C, 59.80; H, 6.69; N, 5.92; Cl, 5.62; Ni, 8.27%. M/S-ESI *m/z* (%): 584 (M + 1 – ClO_4^-). ^{1}H NMR (acetone d6): 8.92 (s, 1H), 8.78 (s, 1H), 8.12 (m, 2H), 8.02 (d, *J* = 3.41 Hz, 1H), 7.69 (d, *J* = 3.41 Hz, 1H) 7.41 (m, 4H), 3.59 (s, 6H), 1.53 (s, 9H), 1.52 (s, 9H), 1.36 (s, 9H). Theoretical calculations were based on Density Functional Theory (DFT) and have been performed with the ORCA program package.[10] Full geometry optimizations were carried out for all complexes using the GGA functional BP86[11] in combination with the TZVP[12] basis set for all atoms by taking advantage of the RI approximation with the auxiliary TZV/J Coulomb fitting basis sets.[13] Increased integration grids (Grid4 in ORCA convention) and tight SCF convergence criteria were used. *g*-Tensors and hyperfine coupling constants were obtained from single-point calculations employing the hybrid functional B3LYP[14] and the EPR-II basis set.[15] Calculations were carried out in a dielectric continuum using the conductor like screening model (COSMO, ε = 9.08) with CH_2Cl_2 taken as the solvent.[16]

1 See the special issue of *Chem. Rev.*, 2003, **103** (6), dealing with radical metalloenzymes.
2 H. J. Krüger, *Angew. Chem., Int. Ed.*, 1999, **38**, 627; B. A. Jazdzewski and W. B. Tolman, *Coord. Chem. Rev.*, 2000, **200–202**, 633; S. Itoh, M. Taki and S. Fukuzumi, *Coord. Chem. Rev.*, 2000, **198**, 3; P. Chaudhuri and K. Wieghardt, *Prog. Inorg. Chem.*, 2001, **50**, 151; F. Thomas, *Eur. J. Inorg. Chem.*, 2007, 2379; F. Thomas, in *Stable Radicals: Fundamentals and Applied Aspects of Odd-Electron Compounds*, ed. R. Hicks, Wiley, Chichester, 2010, pp. 281–316.
3 O. Rotthaus, O. Jarjayes, F. Thomas, C. Philouze, C. Perez Del Vallee, E. Saint-Aman and J.-L. Pierre, *Chem.–Eur. J.*, 2006, **12**, 2293.
4 Y. Shimazaki, F. Tani, K. Fului, Y. Naruta and O. Yamauchi, *J. Am. Chem. Soc.*, 2003, **125**, 10512; T. Glaser, M. Heidemeier, R. Fröhlich, P. Hildebrandt, E. Bothe and E. Bill, *Inorg. Chem.*, 2005, **44**, 5467; O. Rotthaus, F. Thomas, O. Jarjayes, C. Philouze, E. Saint-Aman and J.-L. Pierre, *Chem.–Eur. J.*, 2006, **12**, 6953; Y. Shimazaki, T. Yajima, F. Tani, S. Karasawa, K. Fukui, Y. Naruta and O. Yamauchi, *J. Am. Chem. Soc.*, 2007, **129**, 2559; L. Benisvy, R. Kannappan, Y.-F. Song, S. Milikisyants, M. Huber, I. Mutikainen, U. Turpeinen, P. Gamez, L. Bernasconi, E. J. Baerends, F. S. Hartl and J. Reedjik, *Eur. J. Inorg. Chem.*, 2007, 631; O. Rotthaus, O. Jarjayes, C. Philouze, C. Perez Del Vallee and F. Thomas, *Dalton Trans.*, 2009, 1792.
5 T. Storr, E. C. Wasinger, R. C. Pratt and T. D. P. Stack, *Angew. Chem., Int. Ed.*, 2007, **46**, 5198.
6 M. Orio, O. Jarjayes, H. Kanso, C. Philouze, F. Neese and F. Thomas, *Angew. Chem., Int. Ed.*, 2010, **49**, 4989.
7 M. A. Munoz-Hernandez, T. S. Keizer, S. Parkin, B. Patrick and D. A. Atwood, *Organometallics*, 2000, **19**, 4416.
8 O. Rotthaus, O. Jarjayes, C. Pérez Del Valle, C. Philouze and F. Thomas, *Chem. Commun.*, 2007, 4462.
9 The hyperfine coupling constants A^2_H and A^3_H are assigned to the hydrogens that are in *meta* position of the phenoxyl ring. The computed values are $A^1_H = 25.1$ MHz, $A_N = 16.5$ MHz, $A^2_H = -11.8$ MHz for the more strongly coupled atoms (Table S1, ESI†).
10 F. Neese, *ORCA – an ab initio, Density Functional and Semi-empirical Program Package (v. 2.8–18)*, Universität Bonn, Bonn, Germany, 2007.
11 J. P. Perdew, *Phys. Rev. B*, 1986, **33**, 8822; J. P. Perdew, *Phys. Rev. B*, 1986, **34**, 7406; A. D. Becke, *Phys. Rev. A*, 1988, **38**, 3098.
12 A. Schäfer, C. Huber and R. Ahlrichs, *J. Chem. Phys.*, 1994, **100**, 5829.
13 A. Weigend, *Phys. Chem. Chem. Phys.*, 2006, **8**, 1057.
14 A. D. Becke, *J. Chem. Phys.*, 1993, **98**, 5648; C. Lee, W. Yang and R. G. Parr, *Phys. Rev. B*, 1988, **37**, 785.
15 V. Barone, in *Recent Advances in Density Functional Methods, Part I*, ed. D. P. Chong, World Scientific, Singapore, 1996.
16 A. Klamt and G. J. Schürmann, *J. Chem. Soc., Perkin Trans. 2*, 1993, 799.